

# Matter-Wave Entanglement and Teleportation by Molecular Dissociation and Collisions

T. Opatrný<sup>1,2</sup> and G. Kurizki<sup>1</sup>

<sup>1</sup>Department of Chemical Physics, Weizmann Institute of Science, 761 00 Rehovot, Israel

<sup>2</sup>Theoretical Physics Institut, F. Schiller Universität, Max-Wien-Platz 1, D-07743 Jena, Germany  
and Theoretical Physics Department, Palacký University, Svobody 26, 77146 Olomouc, Czech Republic  
(Received 28 September 2000)

We propose dissociation of cold diatomic molecules as a source of atom pairs with highly correlated (entangled) positions and momenta, approximating the original quantum state introduced by Einstein, Podolsky, and Rosen (EPR) [Phys. Rev. **47**, 777 (1935)]. Wave packet teleportation is shown to be achievable by its collision with one of the EPR correlated atoms and manipulation of the other atom in the pair.

DOI: 10.1103/PhysRevLett.86.3180

PACS numbers: 03.67.Hk, 03.65.Ud, 39.20.+q

The fundamentally profound notion of quantum teleportation is the prescription of how to map, in a *one to one fashion*, any quantum state of system A onto that of a *distant* system B: one must measure the pertinent observables of A, then manipulate their counterparts in B according to the communicated results of the measurements on A [1–7]. Teleportation has thus far been explored for photon polarizations [1–4], optical field quadratures [5,6], and multiatom spin components [7]. Here we pose the basic question: How to teleport the *translational quantum states (wave packets) of material bodies* over sizable distances? We propose dissociation of cold diatomic molecules as a source of atom pairs with highly correlated (entangled) positions and momenta, approximating the original quantum state introduced by Einstein, Podolsky, and Rosen (EPR) [8]. Wave packet teleportation [2] is shown to be achievable by its collision with one of the EPR correlated atoms and manipulation of the other atom in the pair.

Consider a cold beam of ionized molecules that are moving with high, constant velocity  $v_z$  along the  $z$  axis (which thus *plays the role of time*) to a region where they are dissociated by means of an electromagnetic pulse. Let the size  $L$  of the dissociation region along the perpendicular  $x$  axis be defined by means of an aperture (Fig. 1). Here the molecule splits and its two constituents start receding.

In order to be coherent within the dissociation region  $L$ , the translational *center-of-mass* (c.m.) state of the molecule along the  $x$  axis should be close to the minimum uncertainty state (MUS) of its position and momentum, described by a Gaussian  $\exp[-P_x^2/2\Delta P_x^2]$ , where  $P_x$  is the  $x$  component of the c.m. momentum and  $\Delta P_x$  its spread. Such a state can be prepared by translationally cooling the molecules to the ground state of a trapping potential, then ionizing and accelerating them to the required speed  $v_z$  (prior to dissociation). The required temperature is typically  $T \approx \hbar^2/(Mk_B D^2)$ , where  $M$  is the molecular mass,  $k_B$  is the Boltzmann constant, and  $D$ , the c.m. wave packet size, is chosen to be  $D \lesssim L$ . A size  $D \approx 300$  nm would require  $T \approx 3 \mu\text{K}$  for  $\text{H}_2^+$  and  $T \approx 0.4 \mu\text{K}$  for  $\text{Li}_2^-$ .

Such temperatures are achievable by Raman photoassociation of atomic pairs in Bose condensates [9].

We would like the two-atom translational state obtained by molecular dissociation to closely resemble the *original* EPR state [8], whose realization has not been investigated thus far. The perfect EPR state of particles 0 and 1 is described by the wave function  $\Psi(x_0, x_1) = \delta(x_0 - x_1)$ : the positions and momenta of the two particles along  $x$  are completely uncertain, yet perfectly correlated (entangled):  $x_0 = x_1, p_{x0} = -p_{x1}$ . The resemblance of the dissociated

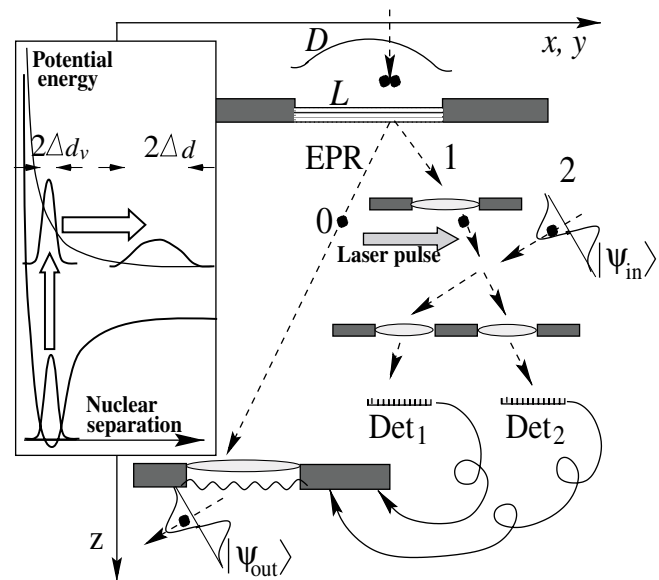


FIG. 1. EPR entanglement and teleportation of atomic wave packets. A cold diatom with c.m. spread  $D$  dissociates into translationally entangled atoms or ions 0 and 1. Particle 1 is focused and laser deflected to collide with particle 2. Their postcollision distance and momentum sum are measured by detectors 1 and 2 and determine the position and momentum shifts of particle 0, whose translational state  $|\psi_{\text{out}}\rangle$  then approximately reproduces  $|\psi_{\text{in}}\rangle$  of particle 2. Inset: short-pulse dissociation yields a replica of the internuclear wave packet on the dissociative potential surface, whose gradient causes the wave packet to spread.

state to the perfect EPR state depends on the extent to which the variances of the correlated atomic variables are *below* the Heisenberg uncertainty limit, so that

$$\Delta x_{01} \Delta P_x \ll \hbar, \quad (1)$$

$\hat{x}_{01} = \hat{x}_0 - \hat{x}_1$  and  $\hat{P}_x = \hat{p}_{x_0} + \hat{p}_{x_1}$  being, respectively, the internuclear separation and c.m. momentum operators. Inequality (1) is possible since the two variances *do not* pertain to canonically conjugate variables. The diatomic molecule prior to dissociation is describable by an internuclear wave packet whose spatial size is  $\Delta d_v$  (typically 0.1 nm), determined by its vibrational state. Dissociation by a short laser pulse can yield an *almost exact replica* of the initial internuclear wave packet on a dissociative electronic potential surface of the molecule (Fig. 1 inset). The much broader, cold c.m. wave packet keeps during dissociation the molecular MUS spread (Fig. 1)  $\Delta P_x \approx \hbar/D$ . As the internuclear wave packet *becomes nearly free* shortly after dissociation, it may still resemble an EPR state. Its proximity to the perfect EPR state at  $t = 0$ , chosen to signify the *completion* of dissociation, can be measured by the parameter  $s$  that is inversely proportional to the left-hand side of (1)

$$s \approx D/\Delta d. \quad (2)$$

Here the width  $\Delta d = \Delta x_{01}(0) > \Delta d_v$  is determined by the dynamical spreading of the internuclear wave packet, caused by the gradient of the dissociative potential surface. The ratio in (2) should be sought to satisfy  $s \gg 1$ , in accordance with inequality (1), the perfect EPR state having  $s \rightarrow \infty$ . Even for the realistic values  $\Delta d \sim 1 \text{ nm} \gg \Delta d_v$ , and  $D \geq 300 \text{ nm}$ , this parameter is remarkably large:  $s \approx 300$ .

There is a noteworthy analogy between the two-particle EPR state and that of entangled two-mode light from parametric down-conversion (PDC) [10,11]:  $s$  is analogous to the exponential of the “squeezing parameter” of such light, which represents the ratio of the standard deviation of the “stretched” field quadrature to that of its “squeezed” counterpart (one quadrature corresponding, e.g., to the sum and the other to the difference of the two fields, analogously to our  $\hat{x}_{01}$  and  $\hbar/\hat{P}_x$ , respectively). In current optical experiments [11]  $s \lesssim 4$ .

Outside the dissociation region (typically, for separations beyond a few nm) the receding particles evolve freely, with diminishing position correlation. Yet the two-particle wave function remains inseparable, having the form  $\Psi(x_0, x_1) = \psi(x_{01})\psi_{c.m.}(x_0 + x_1)$ , i.e., a product of the internuclear wave function and its c.m. counterpart. The spread of the coordinate difference  $x_{01}$  then grows with time as  $\Delta x_{01}^2(t) = \Delta d^2 + \Delta v_{01}^2 t^2$ ,  $\Delta v_{01}$  being the spread of their velocity difference acquired during dissociation (here we assume homonuclear diatomic molecules, for simplicity). Yet the growth of  $\Delta x_{01}(t)$  *can be compensated* by a suitable lens, which *ideally* “time reverses”  $\Delta x_{01}$ , i.e., projects it back to its initial “spot” of size  $\Delta x_{01}(0) = \Delta d$ .

In practice, such compensation is limited by the resolution of the focusing lens (see below).

We suggest that the translationally entangled particles 0 and 1 can be used to demonstrate the *hitherto unobserved* original prediction of EPR [8], concerning the nonlocality of quantum correlations in a free-propagating two-atom state satisfying inequality (1): detecting the momentum or position of particle 1 would make the corresponding variable of particle 0 assume a nearly well-defined value (with fluctuations  $\hbar/D$  or  $\Delta d$ , respectively). By contrast, there will be large fluctuations if we measure *uncorrelated* variables [Figs. 2(a) and 2(b)]: the momentum of particle 1 and the position of particle 0, or vice versa. We note that the preparation of EPR states of *internal atomic observables* (unlike the present external or translational observables) by diatomic dissociation was discussed in [12,13] (for atomic excitations or pseudospin states), and in [14] (for atomic spin states). An EPR correlation of *trapped* (rather than free-propagating) atoms is proposed in [15].

The major challenge is to teleport the quantum state  $|\psi_{in}\rangle$  of the *transversal* motion of particle 2 (along the  $x$  axis) to particle 0 (Fig. 1). To this end, particle 2 collides

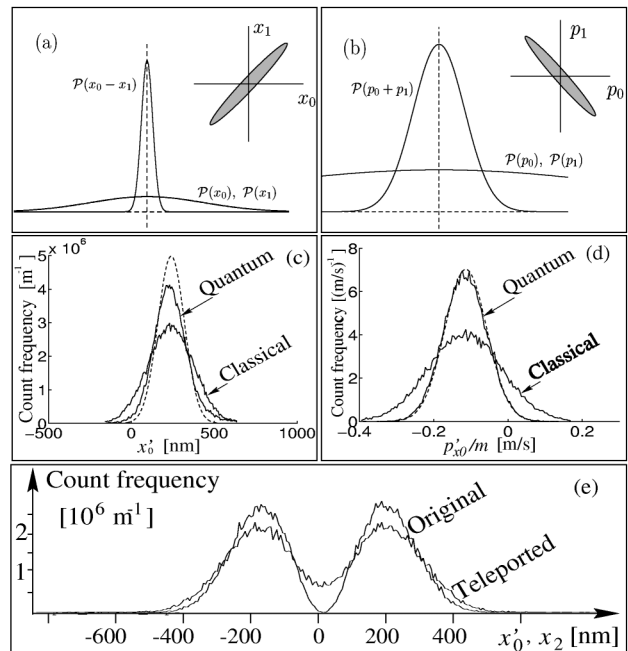


FIG. 2. Probability distributions of the separation  $\mathcal{P}(x_0 - x_1)$  (a) and momentum sum  $\mathcal{P}(p_0 + p_1)$  (b) of the EPR pair, as compared with their respective single-particle counterparts  $\mathcal{P}(x_{0(1)})$  and  $\mathcal{P}(p_{0(1)})$ . (c)–(e) Our prediction for the results of  $5 \times 10^4$  teleportation events with lithium ions with the parameters as in the text. (c) Position, and (d) momentum distribution of a Gaussian wave packet, broken line: ideal input distributions, full lines: results of classical and quantum teleportations (by following classical trajectories of an ensemble obeying the quantum Wigner  $x$ - $p$  distribution). (e) Prediction of the teleported position distribution of a two-peak interference pattern (by applying the calculated teleportation-induced noise to the input distribution).

with one member of the EPR pair—particle 1 (in a synchronous fashion determined by laser pulses—see below), after which both particles 1 and 2 are detected. Essentially, the collision of particles 1 and 2 allows us to project their precollisional *joint state* onto the basis of EPR-correlated states (specified below) and detect the result of the projection. The results of the postcollision detection are used to control the evolution of the “readout” particle 0, the other member of the EPR pair. In the optimal case, the resulting translational state  $|\psi_{\text{out}}\rangle$  of particle 0 would closely imitate the input  $|\psi_{\text{in}}\rangle$  of particle 2. We may assume that  $|\psi_{\text{in}}\rangle$  is prepared by diffraction on a double-slit screen or grating [16]. If measured directly, the beam of particle 2 would exhibit a characteristic diffraction pattern. If the teleportation scheme is applied instead, then the input beam is destroyed but nearly the same diffraction pattern can be observed in the transformed output beam of particle 0. We note that the collision region in Fig. 1 plays an *analogous role to the beam splitter* which mixes a field quadrature of the teleported optical state with the field of one of the entangled PDC modes in the teleportation scheme of [5].

A natural choice for the postcollision correlated (EPR-state) basis is the set of states associated with a sharp (well-defined) sum of the colliding particles’ momenta  $\hat{p}_{x1} + \hat{p}_{x2}$  and sharp difference of their  $x$  coordinates,  $\hat{x}_1 - \hat{x}_2$ . At the time instant  $\tau$ , corresponding to the particles’ nearest approach in the absence of interaction (see below), the operators  $\hat{x}_-$  and  $\hat{p}_+$ , given by

$$\hat{x}_- \equiv \hat{x}_1(\tau) - \hat{x}_2(\tau), \quad (3)$$

$$\hat{p}_+ \equiv \hat{p}_{x1}(\tau) + \hat{p}_{x2}(\tau), \quad (4)$$

are measured, with values  $x_-, p_+$  and precision  $\Delta x_{\text{meas}}$  and  $\Delta p_{\text{meas}}$ , respectively (which are discussed later).

The last step required for the teleportation of the state of particle 2 is the shift of the  $x$  coordinate and momentum of the readout particle 0, according to the inferred values of  $x_-$  and  $p_+$  as  $\hat{x}_0 \rightarrow \hat{x}'_0 = \hat{x}_0 - x_-$ , and  $\hat{p}_{x0} \rightarrow \hat{p}'_{x0} = \hat{p}_{x0} + p_+$ . Let the precision of the position and momentum shifters be  $\Delta x_{\text{shift}}$  and  $\Delta p_{\text{shift}}$ , respectively. From the correlations of  $\hat{x}_0$  and  $\hat{x}_1$ , or  $\hat{p}_{x0}$  and  $\hat{p}_{x1}$  discussed above, we find that (at the relevant times) the shifted variables satisfy

$$\hat{x}'_0 = \hat{x}_2 \pm \Delta x_T, \quad (5)$$

$$\hat{p}'_{x0} = \hat{p}_{x2} \pm \Delta p_T, \quad (6)$$

namely, they approximately *reproduce the teleported variables of particle 2*, to the accuracy given by  $\Delta x_T$  and  $\Delta p_T$  where

$$\Delta x_T^2 = \Delta d^2 + \Delta x_{\text{meas}}^2 + \Delta x_{\text{shift}}^2, \quad (7)$$

$$\Delta p_T^2 = \Delta P_x^2 + \Delta p_{\text{meas}}^2 + \Delta p_{\text{shift}}^2. \quad (8)$$

Equations (5) and (6) imply that the Wigner  $x$ - $p$  distribution  $W(x'_0, p'_{x0})$  of the readout particle 0 is given by that of the input particle 2,  $W_{\text{in}}(x_2, p_{x2})$ , coarse-grained by a

smoothing function whose width is determined by Eqs. (7) and (8).

The teleportation has nonclassical properties provided (i)  $\Delta x_T$  and  $\Delta p_T$  satisfy

$$\Delta x_T \Delta p_T < \hbar, \quad (9)$$

and (ii) they are finer than the scales of the input wave packet variation in position and momentum, respectively [Figs. 2(c)–2(e)]. If the fluctuations produced by the measurements and shifts are negligible ( $\Delta x_{\text{meas}}, \Delta x_{\text{shift}} \ll \Delta d$ , and  $\Delta p_{\text{meas}}, \Delta p_{\text{shift}} \ll \Delta P_x$ ), then the left-hand side of Eq. (9) is approximately  $\Delta x_T \Delta p_T \approx \hbar/s$ . For teleported Gaussian wave packets, the maximum attainable fidelity, i.e., the overlap of the input state with the teleported output, can be shown to be  $F_{\text{max}} = (1 + \Delta x_T \Delta p_T / \hbar)^{-1}$ . As shown in [5], the maximal *classical* teleportation fidelity is 1/2, so that larger fidelity, as in the quantum-optical teleportation experiment [6] where  $F = 0.58$ , attests to quantum correlations. [“Classical teleportation” is based on simultaneous (though noisy) measurements of the noncommuting quantities  $\hat{x}_2$  and  $\hat{p}_{x2}$  and preparing a corresponding MUS wave packet of particle 0.]

We proceed to discuss the experimentally relevant aspects of the envisaged teleportation. The dissociated pairs of fragments (particles) 0 and 1 can be emitted in all directions, but the dissociating field polarization can impose directionality [17]. A significant fraction of the fragment pairs enters the aperture of the lens focusing them onto the region where the collision of particles 1 and 2 takes place. The colliding particles are assumed to be prepared in *uncorrelated* wave packets propagating with the same classical velocity along  $z$ ,  $v_{z1} = v_{z2}$ , and opposite classical momenta along  $y$  (Fig. 3),  $m_1 v_{y1} = -m_2 v_{y2}$ , such that  $v_{z1,2} \gg |v_{y1,2}| \gg \Delta v_{x1,2}$ . Their focusing (and laser-pulse deflection) is such that *in the absence of interaction* the wave packets would cross each other in the  $xy$  plane, where their size would be smallest (“contractive”

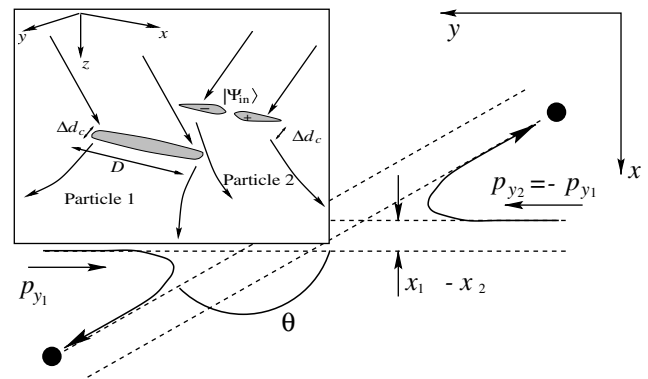


FIG. 3. Collision scheme of particles 1 and 2. Their deflection angle  $\theta$  corresponds to the collision distance  $x_1 - x_2$ . Their momentum sum is conserved. Inset: structure of wave packets 1 and 2, marked by width  $\Delta d_c$  along the  $y$  and  $z$  axes and carrying quantum information along the  $x$  axis.

wave packets [18]). Let us take both particles 1 and 2 to be equally charged. Charged-particle focusing (by electrostatic and magnetic lenses used in high-resolution microscopy) would render the spread (“spot size”) of the colliding particles’ positions as sharp as it was at the relevant times (thus achieving time reversal): for particle 1 this time corresponds to the completion of dissociation, whereas for the teleported particle 2 it is the time of the state preparation (e.g., by a double slit). The arrival of the two particles in the  $xy$  collision plane at  $\tau$  must be *synchronized by laser pulses*, causing the fast switching on of their deflection towards the collision region in the  $x$ - $y$  plane, provided the values of  $z_1$ ,  $z_2$ , and  $v_{z_1} = v_{z_2}$  are appropriate. Synchronization accuracy of  $\sim 10$  ps and  $v_z \sim 10^3$  m/s would bring the particles well within the Coulomb collision range (see below). The  $y$ - $z$  extent of the two wave packets must be  $\Delta d_c \ll D$ , so that they overlap in the absence of Coulomb repulsion (Fig. 3 inset). Among the dissociated atom pairs entering the input aperture  $L$ , only those participating in the *synchronized* collision events are counted as pairs that contribute to successful teleportation.

The success of teleportation hinges upon our ability to discriminate, when detecting the postcollision states, between correlated EPR states with *different values of the relevant parameters*, namely, the parameter  $x_-$  and the momentum sum  $p_+$  in Eqs. (3) and (4). We can infer the parameter  $x_-$  by measuring the relative deflection angle of the colliding particles. A quantitative estimation can be made for repulsive Coulomb interaction of two particles with mass  $m$  and charge  $q$ . Their relative deflection angle is given by (see, e.g., [19])  $\theta = \pi - 2 \tan^{-1}[(x_1 - x_2)/R_{\text{col}}]$ , where  $R_{\text{col}} = mq^2/(4\pi\epsilon_0 p_y^2)$  is the characteristic collision range. To ensure maximal sensitivity of the deflection angle to  $x_-$  it is useful to choose the experimental parameters such that  $\Delta d_c \ll R_{\text{col}} \sim D \sim \max |x_-|$ . From the collisional analysis it follows that the precision of inferring  $x_-$  is mostly affected by the fluctuation of its conjugate momentum component  $\Delta(p_{x2} - p_{x1}) \sim \hbar/\Delta d_v$ . The corresponding resolution of  $x_-$ , obtained from that of  $\theta$ , is  $\Delta x_{\text{meas}} \approx \pi\epsilon_0 \hbar D^2 p_y / (2q^2 m \Delta d_v)$ , provided that  $p_y \geq \sqrt{mq^2/(4\pi\epsilon_0 D)}$ . In particular, for lithium ions with velocities  $v_y \approx 300$  m/s,  $R_{\text{col}} \approx 220$  nm, the resolution of position difference measurements is  $\Delta x_{\text{meas}} \approx 15$  nm. The momentum sum  $p_+$  is measurable by the Doppler shift of Raman transitions induced by two counterpropagating laser fields, with precision better than 1 mm/s [20]. The dominant contribution to its resolution,  $\Delta p_{\text{meas}}$ , then stems from the fluctuation  $\Delta P_x$ , which is, for the given parameters,  $\Delta P_x/m \approx 30$  mm/s.

In the last stage of teleportation, particle 0 must be “kicked” (momentum shifted) and position shifted by ex-

ternal fields. The spread incurred by these shifts is incorporated into Eqs. (7) and (8), and constitutes one of the factors in the anticipated resolution used in the teleportation simulations of Fig. 2(c). Yet the precision of ion optics is currently so high that the dominant contributions in  $\Delta x_T$  and  $\Delta p_T$  stem from  $\Delta x_{\text{meas}}$  and  $\Delta p_{\text{meas}}$ , respectively. We then get for the teleportation of lithium ion wave packets, under the conditions specified above, the estimation  $\Delta x_T \Delta p_T / \hbar \approx 0.08 \ll 1$ . Such spreads would allow for much higher teleportation fidelities of continuous variables than those presently achievable in quantum optical experiments.

The foregoing analysis shows that, despite the challenging nature of the proposed ideas, their experimental implementation does not pose insurmountable (rather than technical) difficulties. The teleportation of matter wave packets by molecular dissociation and collisions is a novel concept, combining elements of molecular dynamics and ion (atom) optics, and having quantum optical analogs. Its realization is a challenging but viable goal to pursue, en route to quantum information exchange between complex material objects.

The support of U.S.-Israel BSF and DFG is acknowledged.

- 
- [1] C. Bennett *et al.*, Phys. Rev. Lett. **70**, 1895 (1993).
  - [2] L. Vaidman, Phys. Rev. A **49**, 1473 (1994).
  - [3] D. Bouwmeester *et al.*, Nature (London) **390**, 575 (1997).
  - [4] D. Boschi *et al.*, Phys. Rev. Lett. **80**, 1121 (1998).
  - [5] S. L. Braunstein and H. J. Kimble, Phys. Rev. Lett. **80**, 869 (1998).
  - [6] A. Furusawa *et al.*, Science **282**, 706 (1998).
  - [7] A. Kuzmich and E. S. Polzik, quant-ph/0003015.
  - [8] A. Einstein, B. Podolsky, and N. Rosen, Phys. Rev. **47**, 777 (1935).
  - [9] R. Wynar *et al.*, Science **287**, 1016 (2000).
  - [10] M. D. Reid and P. D. Drummond, Phys. Rev. Lett. **60**, 2731 (1988).
  - [11] Z. Y. Ou *et al.*, Phys. Rev. Lett. **68**, 3663 (1992).
  - [12] G. Kurizki and A. Ben-Reuven, Phys. Rev. A **32**, 2560 (1985).
  - [13] G. Kurizki, Phys. Rev. A **43**, R2599 (1991).
  - [14] E. S. Fry, T. Walther, and S. F. Li, Phys. Rev. A **52**, 4381 (1995).
  - [15] A. S. Parkins and H. J. Kimble, Phys. Rev. A **61**, 52104 (2000).
  - [16] S. Kunze, K. Dieckmann, and G. Rempe, Phys. Rev. Lett. **78**, 2038 (1997).
  - [17] J. J. Larsen *et al.*, Phys. Rev. Lett. **83**, 1123 (1999).
  - [18] P. Storey *et al.*, Phys. Rev. A **49**, 2322 (1994).
  - [19] B. H. Bransden, *Atomic Collision Theory* (Benjamin/Cummings, Reading, MA, 1983), 2nd ed.
  - [20] M. Kasevich *et al.*, Phys. Rev. Lett. **66**, 2297 (1991).